

This article was downloaded by:

On: 28 January 2011

Access details: *Access Details: Free Access*

Publisher *Taylor & Francis*

Informa Ltd Registered in England and Wales Registered Number: 1072954 Registered office: Mortimer House, 37-41 Mortimer Street, London W1T 3JH, UK



Physics and Chemistry of Liquids

Publication details, including instructions for authors and subscription information:

<http://www.informaworld.com/smpp/title~content=t713646857>

Molecular Dynamics of Binary Fluids in the Region of the Critical Mixing Point: II. The Static and Dynamic Behaviour

Claus Hoheisel^a

^a Lehrstuhl für Theoretische Chemie Ruhr-Universität Bochum, Bochum, Federal Republic of Germany

To cite this Article Hoheisel, Claus(1980) 'Molecular Dynamics of Binary Fluids in the Region of the Critical Mixing Point: II. The Static and Dynamic Behaviour', *Physics and Chemistry of Liquids*, 9: 4, 265 – 284

To link to this Article: DOI: 10.1080/00319108008084781

URL: <http://dx.doi.org/10.1080/00319108008084781>

PLEASE SCROLL DOWN FOR ARTICLE

Full terms and conditions of use: <http://www.informaworld.com/terms-and-conditions-of-access.pdf>

This article may be used for research, teaching and private study purposes. Any substantial or systematic reproduction, re-distribution, re-selling, loan or sub-licensing, systematic supply or distribution in any form to anyone is expressly forbidden.

The publisher does not give any warranty express or implied or make any representation that the contents will be complete or accurate or up to date. The accuracy of any instructions, formulae and drug doses should be independently verified with primary sources. The publisher shall not be liable for any loss, actions, claims, proceedings, demand or costs or damages whatsoever or howsoever caused arising directly or indirectly in connection with or arising out of the use of this material.

Molecular Dynamics of Binary Fluids in the Region of the Critical Mixing Point

II. The Static and Dynamic Behaviour

CLAUS HOHEISEL

*Lehrstuhl für Theoretische Chemie, Ruhr-Universität Bochum,
D 4630 Bochum, Federal Republic of Germany*

(Received November 12, 1979)

In this second part of our report we continue the description of our molecular dynamics (MD) investigations on partially miscible binary fluids near the critical mixing point.¹ Whereas our first article has reported the basic aspects of our attempt to simulate near-critical states, the present paper describes and discusses the entirely calculated results of our simulations.

The three binary fluids, CH₄/CF₄; Ne/Kr; He/Xe have been considered for an MD-simulation including the wider vicinity of the critical mixing point. The thermodynamic and transport properties of these mixtures were satisfactorily reproduced at the region outside the critical point.

Near-critical conditions for the model systems were indicated by an increased correlation length and a slowing down of the relaxation processes. The behaviour of these quantities is in essential accordance with the experimental data for similar near-critical systems.

Changes of the pair-distribution functions showed alterations of the microscopic structure of the systems in the region of the critical point. The self-diffusion coefficients, however, exhibited no anomalies at near-critical conditions according to nmr-measurements on binary liquid systems. Apparently, we have for the first time succeeded in describing theoretically a near-critical state of binary fluids.

1 INTRODUCTION

In continuation of our first paper¹ we present here the results of our molecular dynamics calculations (MDC) for the three binary fluid mixtures CH₄/CF₄ (system I) and Ne/Kr (system II) and He/Xe (system III) based on (12-6) Lennard-Jones (L-J) pair-potentials. The goal and the fundamentals of our studies are discussed at length in part I¹ (see also Ref. 2).

TABLE III

Pressure for system III calculated by MD and the R-K equation of state:

ρ [g/cm ³]	He/Xe ($x_1 = 0.5$)		P_{R-K} [bar]
	T [K]	P_{MD} [bar]	
1.2635	335	815	700
1.3291	315	825	700
1.3645	305	815	700

between these values is satisfactory for the complete concentration range and at various temperatures. We conclude that for the latter systems the simulation is in accordance with experiment, since we believe that the R-K pressures presented in the tables show only negligible deviations from the experimental values (see part I).¹

2.2 Static pair-distribution functions

Due to the three different pair-potentials for the mixtures we have to compute three PDF, $g_1(r)$, $g_{12}(r)$, $g_2(r)$, which are shown for the equimolar composition of the Ne/Kr system in Figure 1.

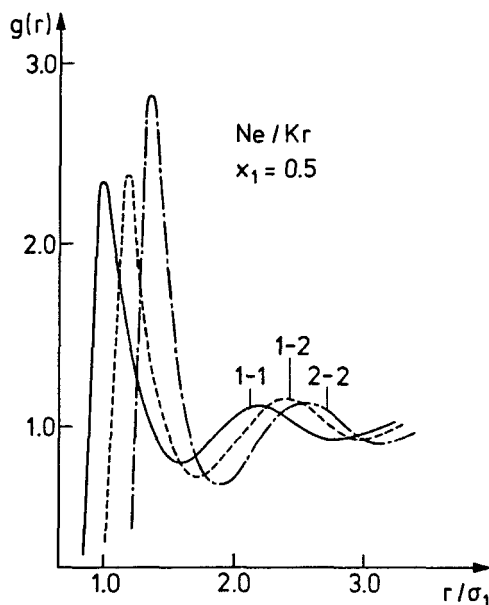


FIGURE 1. Static PDF for an equimolar Ne/Kr fluid mixture: — Ne-Ne, ---- Ne-Kr, - · - · - Kr-Kr.

The positions of the main peaks of these static PDF do not vary with temperature and concentration owing to the relatively fixed average-distances of nearest neighbour particles in liquids. This is however not true for the second and the following maxima of the $g_1(r)$ functions. For these higher coordination shells, the distances between neighbours are more flexible, and variations of the concentration can lead to changes of these distances, i.e. can shift the second peak and higher ones. We display the shifts of the first and the second peak of system II as function of concentration in the Figures 2 and 3. The positions of the peaks of the pure components are chosen as reference values. From the figures we can see that the second line undergoes a remarkable shift, while the first one is constant. Near the critical temperature the situation is not changed for the main line but for the second one, at least in the case of the neon-component. There is a maximum shift at the critical concentration in the case of Ne, and for Kr we observe a constant shift beyond the critical concentration.

The next near neighbours of the same kind appear to alter their distances under near-critical conditions rearranging the liquid structure for the larger molecular distances. This accords with the characteristic increase of the correlation length found in real near-critical† binary systems.

Our calculations on system I may support these results. The methane main peak shifts analogously to the neon peak of system II.³ From the temperature-dependence of the shifts it is additionally derivable that the first line of the methane-component remains essentially constant, whereas the second line exhibits a large shift at the vicinity of the critical temperature.

Studying the molecular structure by means of $g(r)$, we can specifically research the coordination numbers of the coordination shells in liquids. These numbers define the number of, for example, nearest neighbours (1st shell) or of the next near neighbours (2nd shell), which are expected for an arbitrarily chosen molecule of the system. For mixtures we have three of such numbers $n_1^{(k)}$, $n_{12}^{(k)}$, $n_2^{(k)}$ ($k = 1, 2$). The absolute values of these coordination numbers depend on the method applied for their determination. In order to compare absolute numbers, the method of computing these values has to be described.^{4,5}

Here we have evaluated the number of nearest neighbours $n_i^{(1)}$, and that of nearest plus next near neighbours, $n_i^{(2)}$, by integration of the $g_i(r)$ over r up to the first, resp. up to the second minimum.⁶

This way of calculating seems to be most fruitful for MDC, for the minima of $g_i(r)$ are well perceptible in most cases. However, this procedure yields maximum values for $n_i^{(k)}$ often larger than those defined by the cells of a close-packed cubic lattice.⁴

† For the definition of "near-critical" see part I.¹

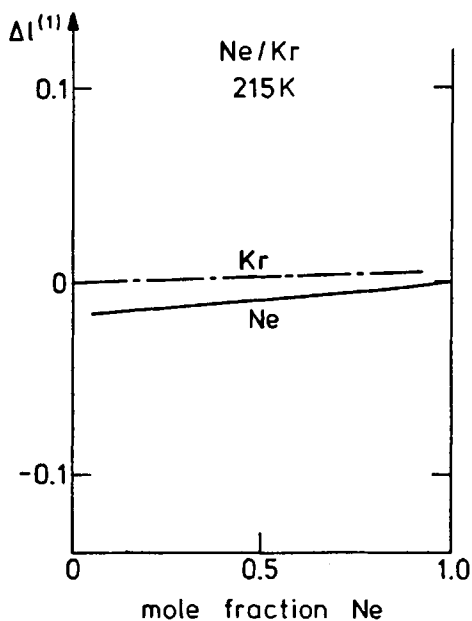


FIGURE 2 Relative shift of the first peak of the static PDF for both components of the Ne/Kr mixture.

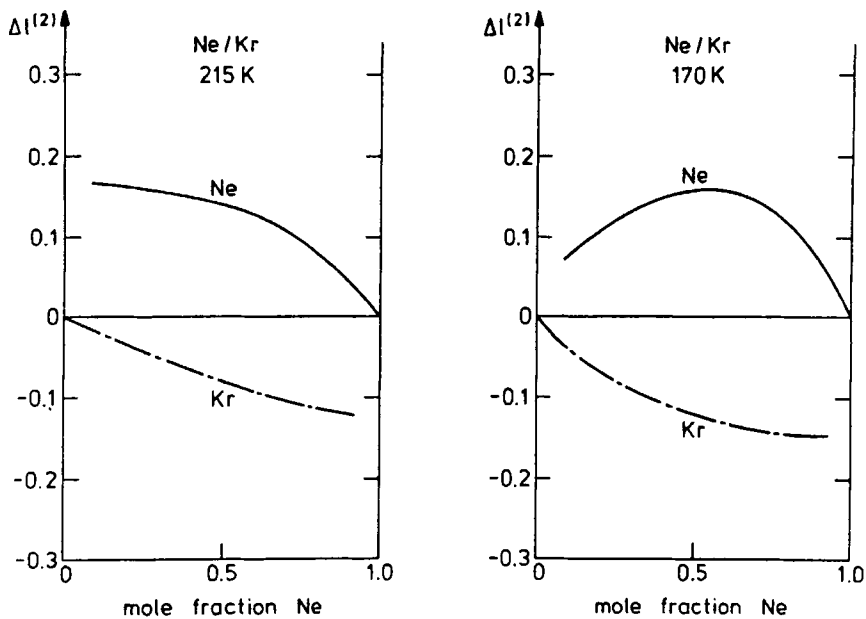


FIGURE 3 As in Figure 2; second peak.

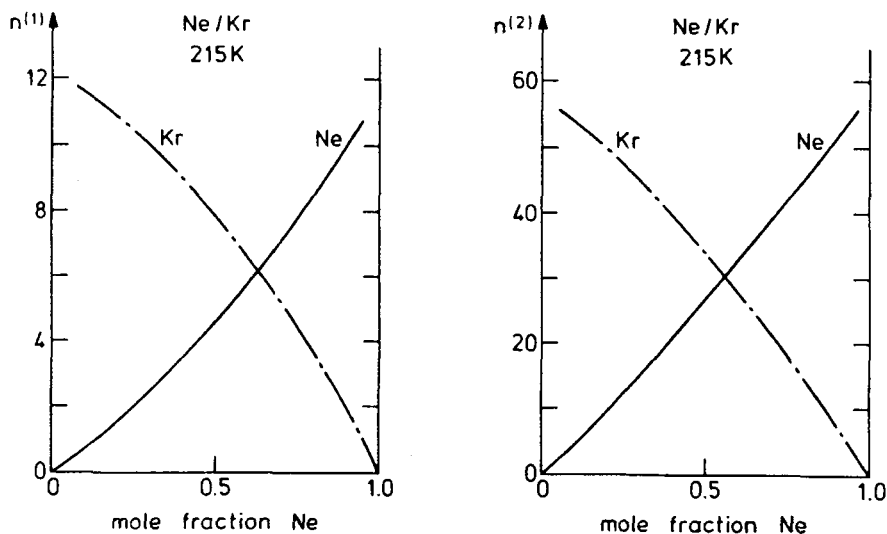


FIGURE 4 Number of neighbours up to the first and up to the second coordination shell for the Ne-Ne and Kr-Kr distributions in the Ne-Kr mixture.

The $n_i^{(1)}$ and $n_i^{(2)}$ calculated as functions of concentration at non-critical temperature for system II are plotted in Figure 4. The curves are graphically drawn from about 30 points each.

As expected for an "ideal mixture," the curves are roughly proportional to the corresponding mole fraction of the components.⁵ With respect to critical conditions the following observations are, however, of interest: For the first coordination shell the neighbour particles of the same species are by no means equally distributed at $x = 0.5$. The point, where the number of neighbours of one species equals that of the other, is obtained by the crossing point of the $n_i^{(k)}$ and the $n_i^{(k)}$ curves, and we shall call it the "equidistribution point" (EDP). This EDP is in this case congruent with the critical composition, $x_1 = 0.63$. The second coordination shell likewise contains different numbers of neighbours at $x = 0.5$, but here the EDP has already decreased to $x_1 = 0.55$. That is, for this non-ideal mixture the number-ratio of the neighbours reaches the total mole fraction of the mixture only within the higher coordination shells. In the above example, we may certainly expect that the EDP occurs at $x_1 = 0.5$ for the third coordination shell ($k = 3$), though we have not attempted to perform detailed calculations on this.⁵

The results on system I show an analogous behaviour of the $n_i^{(k)}$, although only the temperature-dependence is investigated. From Figure 5 it can be seen that $n_1^{(1)}$ falls in line with $n_2^{(1)}$ within the error-bars of that calculation, indicating the equal distribution at critical concentration. The right-hand side diagram of Figure 5 additionally shows that $n_2^{(2)}$ is always lower than

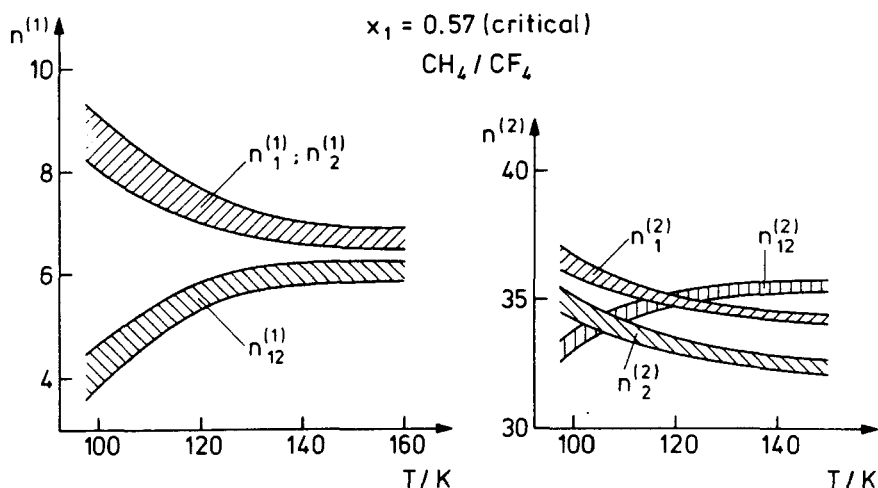


FIGURE 5 Number of neighbours up to the first and up to the second coordination shell for the CH_4 - CH_4 and the CF_4 - CF_4 and the CH_4 - CF_4 distributions in the CH_4/CF_4 mixture.

$n_1^{(2)}$: the EDP is shifted. Our calculations on system III also support these findings.

Explanations for this are offered by considering the very different energy potential functions of the molecules involved in the mixture. Specifically, the differences pertaining to the volume parameters generate non-proportional distributions within the lower coordination shells. In other words: the higher the volume-differences of the component molecules, the higher the deviation of the local particle number ratio of the lower shells from the total mole fraction of the system.⁷

It is furthermore likely, that the EDP is an appropriate starting point for a binary system to aggregate clusters of particles of the same species, since both kinds of molecules have already the maximum number of particles of their own kind as nearest neighbours. A mixture with this equidistribution seems to be more apt to become critical than mixtures of other compositions. In view of this it is reasonable that for partially miscible binary fluids the critical concentration falls in line with the EDP of the first coordination shell.

For the near-critical temperature of 170 K we have calculated diagrams similar to those presented in Figure 4. However, the concentration value of the EDP of the second coordination shell shifts with temperature. Unfortunately the diagrams could not be established for a row of temperatures, since the computing time is extremely large for only one of the diagrams. To cope with this problem we accurately calculated the diagrams for 215 and 170 K only and carried out a few calculations with less accuracy to determine approximately the EDP at 230 and 200 K. We display in Figure 6 the

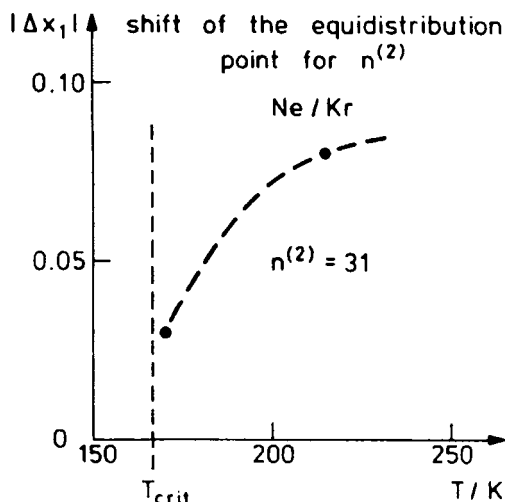


FIGURE 6 Shifts of the EDP for the second coordination shell.

relative shift of the EDP of the next near neighbours as function of temperature. The relative shift is measured as the positive difference of the mole fractions of the $n^{(1)}$ -EDP and the $n^{(2)}$ -EDP. It is evident from this Figure 6, that near the critical temperature the shift is small, whereas for non-critical temperatures it is appreciably large. That is, for non-critical states the ratio of neighbours of the second coordination shell resembles already to what is expected from the total mole fraction of particles of the system. In contrast to this, for the near-critical state the ratio of $n_1^{(1)}$ and $n_2^{(1)}$ still persists to the second shell, and is thus considerably removed from that of the total concentration in this case, $x_1 = 0.63$. The system shall therefore need the higher coordination shells to reach the ratio of neighbours proportional to the total mole fraction. This spatially extended structure of the $g(r)$ functions characterizes the increased coherence length of the system at near-critical temperature.⁸

From these results we attempted to derive an estimation of the coherence length for non-critical and near-critical conditions. We applied two methods, which generated values in good agreement of each other. Firstly, the concentration-shift of the EDP was extrapolated to the total concentration; secondly, the local concentrations in the coordination shells computed with respect to the $n_{1/2}^{(1)}$ and $n_{1/2}^{(2)}$ values were extrapolated to the total mole fraction of the system.

Obeying the first procedure we plotted the concentration coordinate of the EDP of $n^{(k)}$ against the order (k) of the pertaining coordination shell. The extrapolation towards equimolar concentration, $x = 0.5$, then indicated the required number of the shell, i.e. the corresponding radius as correlation

length of the system. We carried out this extrapolation for 200 K (non-critical) and 170 K (near-critical). Referring to the second more reliable method the local mole fractions of the numbers of neighbours of both kinds of molecules, defined as

$$\frac{n_1^{(k)}}{n_1^{(k)} + n_{12}^{(k)}}$$

and

$$\frac{n_2^{(k)}}{n_2^{(k)} + n_{21}^{(k)}} ,$$

were drawn versus the order of the pertaining shell (k).

Linear extrapolation to the critical concentration, $x_1 = 0.63$ ($x_2 = 0.37$), then yielded the order of the shell, i.e. the correlation length we were interested in. This second method was applied to the non-critical and near-critical state, but was additionally used for both components. The coherence length ξ resulting from method 1 was in essential agreement with the two values of ξ derived from method 2. ξ is about 10 Å for the non-critical state and about 30 Å for the near-critical state. The fairly large values of ξ at non-critical temperatures seem to be justified due to the very different molecules contained in this system (see above).

Assessing the approximation of the "pseudo-critical" temperature T_c^P of the model system to be about 2 K, we obtain an increase of the coherence length by a factor of 3 when lowering the temperature from $T_c^P + 40$ to $T_c^P + 2$ K.

The tendency of an expanding coherence length depending on the approximation of the critical temperature agrees with results of scattering experiments on binary liquid systems. Most of these measurements have been performed at the immediate vicinity of a critical point, and here an increase of a factor 10–1000 is ascertainable.⁹

There exist, however, a few experiments for the near-critical region, which are already reported in part I.¹ Those experimental results are in excellent accordance with our data from MDC. The correlation length of the liquid system Aniline/Cyclohexane is enlarged by about a factor 5 (varying from 8 Å to 42 Å) when T is altered from $T_c + 40$ to $T_c + 2$ K.¹⁰

The agreement is in fact enhanced, if one correctly takes the relative parameter $\kappa = (T - T_c)/T_c$ instead of $T - T_c$. For a decay of κ from 0.176 to 0.0117, the experimental and the model system display the same increase of ξ of about the factor 3. Pertaining to both the absolute values of ξ and the relative increase, a better accord cannot be expected including the many assumptions involved in our estimation of ξ : the extrapolation from only

two values is not very reliable, although, on the other hand, this extrapolation seems more reasonable for the model system than that including the third peak of the PDF, since we already have to consider "rounding" effects for the third peak of the PDF of our finite model system. Nevertheless, the linear extrapolation is certainly a rough procedure: first, for non-critical conditions, $g(r)$ disappears exponentially, second, near a critical point $g(r)$ decays proportionally to $1/r$ for large r , as is derivable by theoretical considerations (see part I).¹ With respect to our other approximations we have however avoided applying exponential or hyperbolic extrapolations.

The results on system I do not have the accuracy sufficient for similar extrapolations. For system III, we are now in the process of calculating ξ by another, more precise method.

In addition to these changes within the larger neighbourhood of the molecules, we have revealed changes of the short range order of the particles at near-critical temperature for all the model systems considered. Figure 7 and the left hand side diagram of Figure 5 show the number of nearest neighbours as functions of temperature for system I and system II. For system I we have given the data in form of interval areas illustrating the estimated error-bars. From both plots, however, it is evident, that by approaching the critical temperature the number of nearest neighbours of the same kind of particles $n_i^{(1)}$ rises appreciably. Attention must be paid to the fact that $n_1^{(1)} = n_2^{(1)}$ at critical concentrations! Figure 5 additionally contains the $n_{12}^{(1)}$. In contrast to $n_1^{(1)}$ and $n_2^{(1)}$ this number decreases approaching the critical temperature. For the systems II and III the decay of $n_{12}^{(1)}$ was also noticeable, but not so distinct.

Our theoretical indication of the preference of like pairs of particles

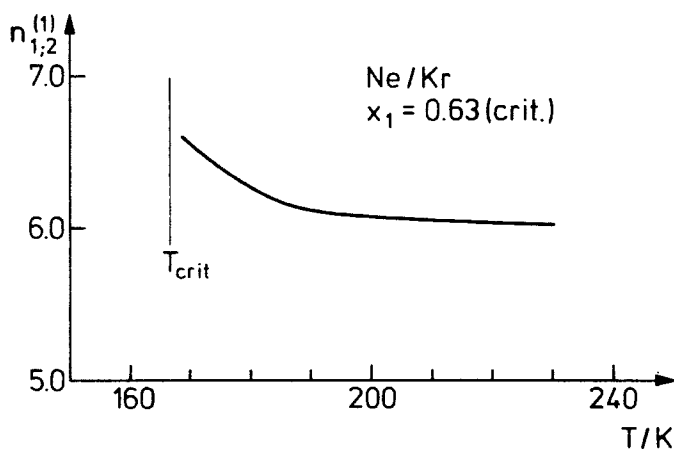


FIGURE 7 Number of nearest neighbours for the Ne-Ne and Kr-Kr distributions.

among unlike pairs supports results of nmr-measurements on the binary liquid mixture Aniline/Cyclohexane at the vicinity of the critical solution point.¹¹ The authors of this study had concluded somewhat speculatively, that there is a statistical predominance of like pairs over unlike pairs for the critical mixture.

Apparently our findings disagree with the common opinion that the short range order of the molecules is not affected by critical conditions.¹² To enlighten this point experimentally it would be worthwhile to study binary systems quantitatively at the vicinity of the critical point by x-ray and neutron scattering experiments.

3 THE TIME-DEPENDENT PROPERTIES OF THE MIXTURES

3.1 Self-diffusion coefficients (SDC)

We have calculated the SDC of both components depending on concentration and temperature for all three systems.³ Herein we will only be concerned with the temperature dependence of these quantities, D_1 and D_2 , at constant critical composition of the mixture. In Figure 8 we display, for example, the D_i of system II plotted in a logarithmic scale against the inverse temperature. The SDC show the expected linear feature, in fact, also near the critical

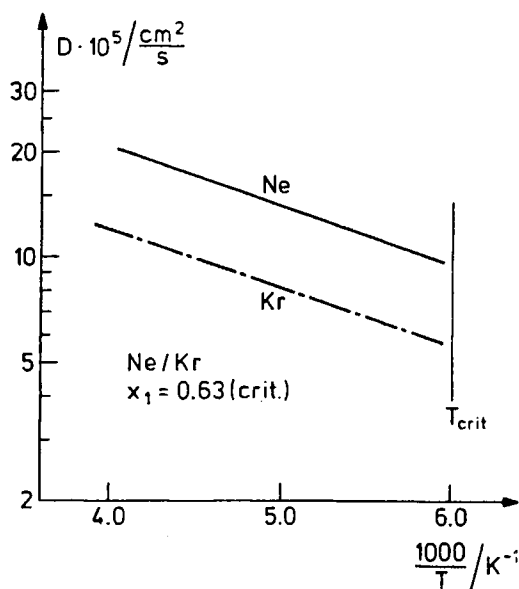


FIGURE 8 SDC of the components of the Ne/Kr mixture.

temperature. These results on system II are essentially in accordance with those on systems I and III. Unfortunately there are no experimental SDC available for any of the components of these mixtures in the thermodynamic region considered here. Nevertheless, it is possible to estimate these SDC values for the non-critical range from data of the pure substances. From these considerations it seemed to be likely that our theoretical values for the model mixtures lie within the interval of the values expected for the real fluid mixtures. This is true for all the systems. We shall, however, not repeat the arguments here.⁵

The behaviour of the theoretical SDC exhibits no anomalies near the critical mixing point of all three systems. This normal temperature dependence of the SDC in the vicinity of the critical solution temperature has experimentally been found for various liquid mixtures. In contrast to contradictory measurements on pure liquids^{13,14} for mixtures, the ordinary temperature dependence near the critical point has been measured.^{15,16} The results of our MDC support these measurements on mixtures for the near-critical region. They should, however, not be used for conclusions concerning the direct neighbourhood of the critical point.¹⁷

3.2 Dynamic pair-distribution functions

In MDC the self-term G_s and the distinct-term G_d of the dynamic PDF are separately available.^{1,18} Since G_s essentially governs the self-diffusion process of the system, and we have not obtained any indication of an anomalous behaviour of the SDC near the critical point, we only attempted to determine $G_d(r, t)$ from our calculations. For simplicity we shall leave out the subscript d in the subsequent text.

Evaluating the three dynamic PDF G_1, G_{12}, G_2 was one of the extensively computer time consuming steps of our calculations. Thus we performed these computations for system II only and considered the temperature dependence at the critical concentration. Furthermore the time dependence of G was studied at only three distinct times:

$$t_1 = 0, \text{ s}, \quad t_2 = 0.5 \cdot 10^{-12} \text{ s}, \quad t_3 = 1.2 \cdot 10^{-12} \text{ s}.$$

The functions, on the other hand, have been determined with the highest accuracy, to date available for such a kind of computation. All the MDC on these functions were done with an 864-particle ensemble and a "cut-off distance" of $r_c \geq 3.3\sigma_1$. The mean-deviation can be estimated to be 1–2%.

The plots on Figure 9 illustrate the spatial and time-dependent decay of $G_1(r, t)$ for near-critical conditions. These plots are drawn from 40–80 points each.¹⁹ For reasons of technical details of our program, we omitted the range of small r -values. However, for t sufficiently large, the $G(r, t > 0)$ function

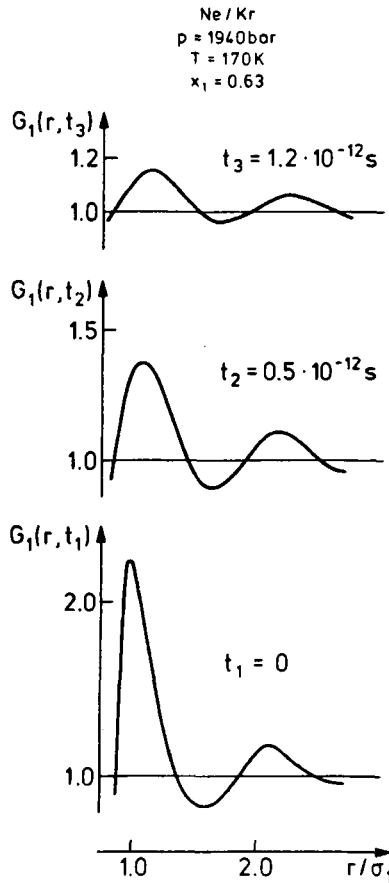


FIGURE 9 Dynamic PDF for a near-critical state of the Ne/Kr mixture.

shows positive values, even at r -values, where $G(r, t = 0) = g(r)$ is already zero.²⁰

A simple and sound method of studying time-dependent correlations within the coordination shells of the liquid system is devised by recording the time-dependent decay of the amplitudes of the $G_i(r, t)$ -peaks. We have studied this decrease for the first two lines of all the $G_i(r, t)$ functions depending on the approach of the critical temperature. For a non-critical temperature the time-decay of the peak-amplitudes is displayed in Figure 10. In comparing the time-decay of the maxima at the different temperatures, we observed a particular behaviour of the second peak. The amplitude of the second peak shrinks very little with time in the near-critical range. The main peak behaves similarly near the critical point, but not so distinctly. To emphasize

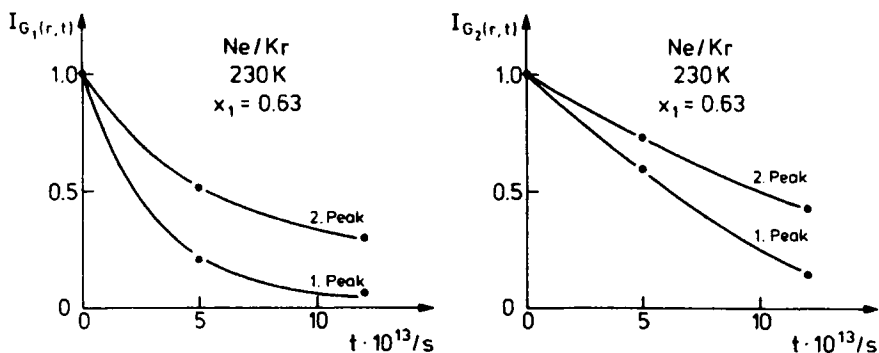


FIGURE 10 Normalized time-decay of the peak-amplitude of the dynamic PDF at non-critical temperature of system II for both components.

this strongly altered time-behaviour of the second peak, we have plotted relative half-lives of the amplitudes versus the temperature on Figure 11. The relative half-life $\Delta t_{1/2}$ is defined as half-life of the amplitude of the second peak scaled by that of the first peak.

From Figure 11 it can be seen that $\Delta t_{1/2}$ rises appreciably in the near-critical region, although these *relative* half-lives are plotted only. For both components the values at 170 K are enlarged by more than a factor two compared to those at the non-critical temperature of 230 K.

Apparently the characteristic time-constant of the system grows sharply in the near-critical region. These results go parallel with experimental find-

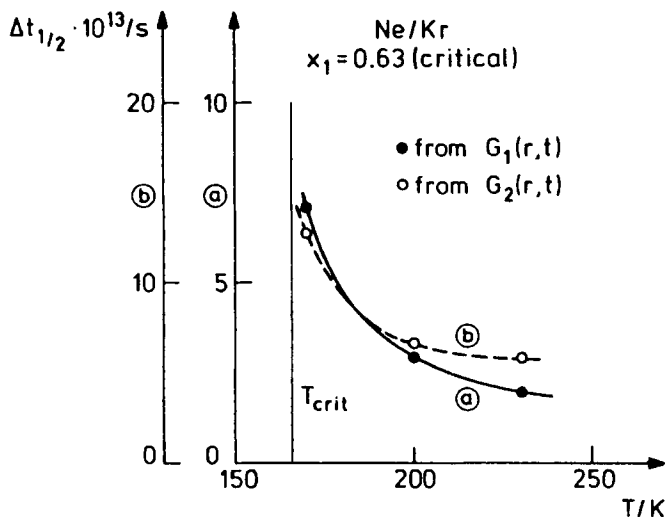


FIGURE 11 Relative half-lives of the amplitude of the second peak of the dynamic PDF for both components of system II.

ings on other critical systems, where a remarkable slowing down of the relaxation processes, the so-called "critical slowing down" has been ascertained.²¹

The characteristic time-constant of the system, i.e. the correlation time of the particles usually increases with decreasing temperature due to the higher density, i.e. the denser packing of the molecules. However, at liquid-like densities, this increase is small, as is confirmed by our model calculations for non-critical temperatures from 230 K to 190 K. Moreover, this natural temperature dependence of the half-lives should be largely eliminated by taking the relative values.

The positions of the maxima of the $G_i(r, t)$ -lines shift with time, as can be seen from Figure 9. We present these line-shift relative to the reference line at $t_1 = 0$ in Figure 12. The shift can be ascribed to the variation of the distribution of particles, which becomes more uniform, more gaussian, as time passes. The peaks change into a symmetric form varying the positions of the maxima.¹⁹

Our investigations of these shifts yielded results indicating that the peak-positions vary only little at the near-critical range in contrast to the non-critical range. The positive relative shifts referred to the shift at 230 K and for an intermediate time-interval of $8 \cdot 10^{-13}$ s are presented in Figure 13 as function of temperature. For both components, these relative shifts go parallel to the curves of the half-lives, increasing noticeably, when the critical temperature is approached. Comparing the plots of the Figure 11 and Figure 13 we have, however, to pay attention to the following facts:

1) The shifts were not obtained as precisely as the peak-amplitudes. Because of the broadness of the $G(r, t)$ -peaks the positions of the maxima were often not quite certain. Therefore the plots on Figure 13 essentially indicate the trends of the shift.

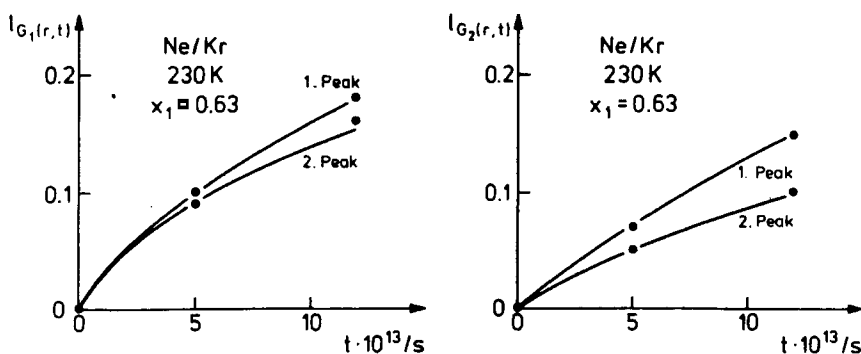


FIGURE 12 Time-dependent line-shifts of the dynamic PDF at non-critical temperature of system II for both components.

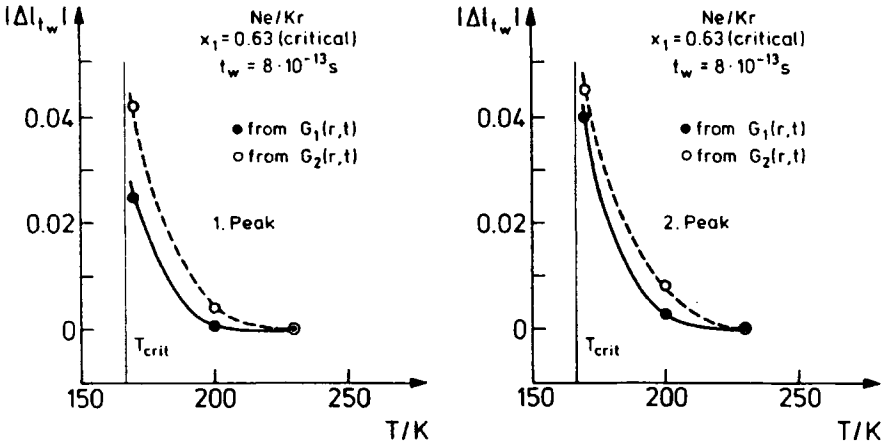


FIGURE 13 Relative line-shifts of the dynamic PDF. The relative shifts have been obtained as difference values, where the positions of the $G_i(r, t)$ -peaks at 230 K are taken as reference. Time-interval: 8×10^{-13} s.

2) The absolute values of the shift nearly disappear in the vicinity of the critical temperature. In order to obtain the relative values we have designated the position of a computed maximum of a specified $G_i(r, t)$ peak as $q(t, T)$ indicating the time- and temperature-dependence. Bearing in mind that our observation-time-interval is $t_w = 8 \cdot 10^{-13}$ s and our reference temperature is $T_{st} = 230$ K, we subsequently get the relative shift from the following relation:

$$\Delta T_{i,w} = (q(t_w, T) - q(0, T)) - (q(t_w, T_{st}) - q(0, T_{st}))$$

3) In contrast to Figure 11 the drawings in Figure 13 involve the “natural shift” depending on the temperature, i.e. on the density of the system. So the steeper increase of the curves in Figure 11 seems to be reasonable.

Our investigations on the line-shifts are entirely consistent with the findings on the peak-amplitudes. They indicate an anomalous growth of the correlation time in the near-critical region of the model system. This is essentially in accordance with measurements of the relaxation time of fluids and magnetizeable systems.^{21,22}

Our MDC on these time-dependent phenomena show, similar to the computations of the static quantities, that the higher coordination spheres are predominantly affected by near-critical conditions, but in addition the short-range order of the system is changed.⁵

Complementary calculations for the $G_{12}(r, t)$ PDF have not led to new results. The time-dependence of these functions is analogous to those of G_1 or G_2 , significant changes could not be revealed.

We have also attempted to evaluate the number of neighbours within the first two coordination shells. Unfortunately, reliable results for it were not available from MDC, since the required minima could not be determined with satisfactory precision. Consequently we have tested another method of calculating the $m_i^{(k)}$, however, these values were not comparable to the $n_i^{(k)}$ of the static PDF, and we refrained from interpreting them.

3.3 Characteristic time constants

To date for this or similar systems, there exists no experimental study of the dynamic structure factor $S(k, \omega)$ satisfactorily extended to the k -region, which we are interested in to derive the decrease of the characteristic frequency for the near-critical region. The measurement of dynamic properties is difficult, and is therefore performed only for a small (k, ω) -range and often very close to the critical point.

Our comparisons with experimental and other theoretical work thus can only reveal the general trends. In order to obtain an estimation of the “near-critical slowing down” of our model system, we have chosen the disappearing of the second peak of $G_1(r, t)$ with time as a measure for t_c . The time decay of the second maximum of $G_2(r, t)$ is much slower and provides no reasonable extrapolation. In this way we obtained in terms of linear extrapolations towards zero-amplitude the ratio

$$\frac{t_c^{\text{near-crit}}}{t_c^{\text{non-crit}}} \approx 4 \quad \text{with} \quad \eta^{\text{near-crit}} = \frac{T^{\text{near-crit}}}{T_c} = 1.02$$

and $\eta^{\text{non-crit}} = 1.25$.

From light scattering experiments the characteristic frequency $\omega_c = 1/t_c$ is available from the half-width of the Rayleigh peak which is extremely narrowing close to the critical point. This frequency ω_c falls by a factor 10–20, when η is lowered from $\eta = 1.10$ to $\eta = 1.01$.²³ A similar steep decay is predicted from theoretical work on a ferro-electrical solid system for a change of η from 1.4 to 1.05.²⁴

Hence it appears that our model system exhibits approximately a “slowing down” fairly comparable to experimental systems in the vicinity of the critical point.

Ideally we wish to extrapolate critical exponents from our MDC to base the comparisons with experimental data on these numbers. However, to do so, we have to know precisely the pseudo-critical point of our model mixture and we necessarily have to perform computations very near to this point. Neither was possible within our present calculations. We believe, however, that it can be achieved, if additionally the specific heat of the system is calculable.²⁵

4 Discussion and conclusions

The present results of our model calculations shall finally be discussed in terms of the following two aspects:

- a) To what extent we have succeeded in simulating the "real" mixtures by the models: far away, and fairly close to the critical mixing point.
- b) Which forthcoming results for the near-critical states could be obtained by these computations.

One assumption for a successful simulation of a mixture is the satisfactory model-description of the corresponding pure fluids. We have accomplished this condition for the systems II and III completely, for system I partly. It is obvious that this exclusively holds for the thermodynamic region considered here.

The properties of the model systems agreed satisfactorily with those of the experimental ones at non-critical conditions. Near-critical conditions for the model systems were expected for the region of the pertaining experimental systems. The increase of the coherence length and the characteristic time-constant as well as changes of the microscopic structure of the model system clearly indicated the vicinity of the pseudo-critical state.

Further indications on the fact that the present calculations have simulated near-critical states can be drawn from two additional assessments:

Firstly, an anomalous increase of the number of nearest neighbours by approaching the experimental mixing temperature could **not** be observed in MDC at non-critical compositions.

Secondly the MDC far below the critical temperature within the experimental two-phase region of the systems either did not converge to a stationary state or led to badly reproducible results for all concentrations near the critical one. Nevertheless, we tried to derive the tendencies of the behaviour of the SDC and PDF at this region. From pilot-calculations on system I we obtained a different slope for the $(\log D - 1/T)$ -plot in this range compared to that in the homogeneous region. Furthermore, the correlation length of the system II and III as well as characteristic time constant seemed to be smaller in this region than near the critical point within the homogeneous part of phase diagram. The values tended to approach the level which had been computed for the non-critical region far above the critical point.

Further evidence showing that the model system is really studied at the vicinity of the critical phase separation has been worked out through the approximate calculation of the Gibbs energy of the model system II. We have, in detail, described the main features of this calculation method in Ref. 5. However, the results are graphically repeated in Figure 14. The characteristic term of the molar Gibbs energy of the mixture is plotted

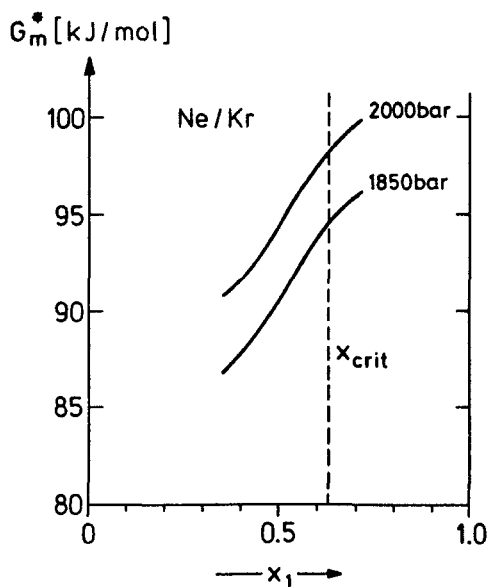


FIGURE 14 Molar Gibbs energy G_m^* (see Ref. 5) versus x_1 at 165 K.

against the concentration at a constant temperature of 165 K and two near-critical pressures. In the region of the critical composition the plotted function exhibits a curvature concave to the x -axis, which characterizes phase separation of a binary liquid mixture.²⁶ For a temperature of 170 K, in turn, the concave curvature of the functions nearly vanishes. This points to the homogeneous region of the system. The 170 K curves were calculated with lesser accuracy and were therefore not included in Figure 14.

With respect to all our comparisons and assessments we conclude that the present model calculations have simulated near-critical states for binary fluid systems on the basis of L-J effective pair-potentials. Forthcoming MDC on system III will be applied to evaluate critical indices, at least for the static quantities.

Though the experimental determination of the quantities calculated herein will involve essential difficulties, direct experimental evidence for our theoretical findings could be achieved by modern x-ray and neutron scattering measurements on these or similar systems.

As one remarkable result of our theoretical studies it turned out that the short-range order in a mixture is significantly affected by near-critical conditions. These changes seem to be small, but were discovered for all the systems. It is hard to believe that these results could ensue artificially from the microscopic size of our systems, for especially the first coordination shell should not be affected by "rounding" as long as the correlation length

is not considerably enlarged very close to the critical point. In connection with this, it is interesting to investigate the alterations of the short-range order of fluids at the direct vicinity of the critical point.

We hope and expect that in the future much larger systems may be handled by molecular dynamics to enable us to study fluids very close to a critical point, too.

Acknowledgements

The author thanks Prof. Dr. W. Kutzelnigg for his consistent support of this work. He is further indebted to Dr. U. Deiters, who has contributed both through his own calculations and valuable discussions. The work has furthermore been improved by substantial advice and suggestions of Prof. Dr. F. Kohler.

Most of the calculations have been done on the TR 440 computer of the Rechenzentrum der Ruhr-Universität Bochum and on the minicomputer Interdata 8/32 sponsored by the Deutsche Forschungsgemeinschaft.

References

1. C. Hoheisel, *Phys. Chem. Liquids*, **9**, 245 (1980).
2. C. Hoheisel, *Habilitationsschrift Bochum*, 1979.
3. C. Hoheisel, *Ber. Bunsenges. Phys. Chem.*, **81**, 462 (1977).
4. J. S. Pings, *Physics of Simple Liquids*, edited by H. N. V. Temperley, J. S. Rowlinson, and G. S. Rushbrooke (North-Holland), 1968.
5. C. Hoheisel and U. Deiters, *Molec. Phys.*, **37**, 95 (1979).
6. A. Rahman, *J. Chem. Phys.*, **45**, 2585 (1966).
7. K. Nakanishi and K. Toukubo, *J. Chem. Phys.*, **70**, 5848 (1979).
8. M. E. Fisher, *Rev. Mod. Phys.*, **46**, 597 (1974).
9. A. Münster and K. Sagel, *Ber. Bunsenges. Phys. Chem.*, **62**, 1075 (1958).
10. B. Volochine, *Ber. Bunsenges. Phys. Chem.*, **76**, 217 (1972).
11. J. E. Anderson, and W. H. Gerritz, *J. Chem. Phys.*, **53**, 2584 (1970).
12. S. H. Chen, *Physical Chemistry: An Advanced Treatise*, VIII A, edited by H. Eyring, D. Henderson, and W. Jost (Academic Press), 1971.
13. J. S. Duffield and M. J. Harris, *Ber. Bunsenges. Phys. Chem.*, **80**, 157 (1976).
14. K. R. Harris, *Physica*, **93A**, 593 (1978).
15. C. Hoheisel and H. Richtering, *Z. Phys. Chem. N.F.*, **55**, 323 (1967).
16. H. Hamann, C. Hoheisel, and H. Richtering, *Ber. Bunsenges. Phys. Chem.*, **76**, 249 (1972).
17. M. Gittermann, *Rev. Mod. Phys.*, **50**, 85 (1978).
18. B. J. Berne, *Physical Chemistry: An Advanced Treatise*, Vol. VIIIb, edited by H. Eyring, D. Henderson, and W. Jost (Academic Press), 1971.
19. C. Hoheisel, *Molec. Phys.*, **38**, 1243 (1979).
20. A. Rahmann, *Phys. Rev.*, **136A**, 405 (1964).
21. H. E. Stanley, G. Paul, and S. Milosevic, *Physical Chemistry: An Advanced Treatise*, VIIIb, edited by H. Eyring, D. Henderson, and W. Jost (Academic Press), 1971.
22. P. C. Hohenberg and B. J. Halperin, *Rev. Mod. Phys.*, **49**, 435 (1977).
23. P. Berge, P. Calmettes, C. Laj, M. Tournarie, and B. Volochine, *Phys. Rev. Lett.*, **24**, 1223 (1970).
24. N. Ogita, A. Oeda, R. Matsubara, H. Matsuda, and F. Yonezawa, *Phys. Soc. Jap.*, **26**, 145 (supplement), (1969).
25. H. J. M. Hanley and R. O. Watts, *Physica*, **16**, 351 (1975).
26. R. Haase, *Thermodynamik der Mischphasen* (Springer Verlag), 1956).